TWO–POINT RAY TRACING AND CONTROLLED INITIAL–VALUE RAY TRACING IN 3-D HETEROGENEOUS BLOCK STRUCTURES

Petr Bulant

Department of Geophysics, Charles University, Ke Karlovu 3, 121 16 Praha 2, Czech Republic, E-mail: bulant@seis.mff.cuni.cz

Summary

New routines of the two–point ray tracing program, which connect two-point ray tracing with controlled initial–value ray tracing, are discussed. Examples of two–point ray tracing in 3-D are given.

1 Introduction

The *shooting method* is based on iterative application of an *initial–value ray tracing* algorithm. The existing version of the shooting algorithm was designed for two–point ray tracing in considerably general 3-D models of heterogeneous geological structures. In each computation, only the rays of a single *elementary wave*, i.e. the rays whose behaviour at structural interfaces is prescribed by a priori information called the *ray code*, are considered. The rays are thus specified uniquely by the *ray take–off parameters*. For each given ray code, the principal problem of two–point ray tracing in heterogeneous block models then consists in a sufficiently accurate determination of the boundaries between rays with different *ray histories*, i.e. passing through different geological blocks, across different structural interfaces, terminated in different areas for different reasons, or passing through a different number of caustics. The demarcation belts between the different ray histories, corresponding to the numerical uncertainty of the boundaries between the ray histories, have to be kept reasonably narrow, because all two–point rays, situated inside the demarcation belts, will be lost. Once the 2-D domain of ray take–off parameters, the *ray domain,* is decomposed with given accuracy into *homogeneous subdomains* corresponding to rays of equal ray histories, the two–point rays can be found (using, e.g., the paraxial ray approximation) within the individual homogeneous subdomains corresponding to *successful rays* (rays passing through the *reference surface* at which the receivers are situated).

The corresponding Fortran 77 computer code for 3-D two–point ray tracing was developed on the basis of package `MODEL` to specify *smooth block models* of geological structures, and package `CRT` for initial–value ray tracing in such models (Červený *et al.* 1988). The two–point ray tracing code was described in detail in Bulant 1995a and Bulant 1996. In this paper we shall briefly remind the reader the most important steps of the two–point ray tracing algorithm, and discuss the new routines of the two–point ray tracing code, which connect two–point ray tracing with controlled initial–value ray tracing. Finally, two numerical examples of the two–point ray tracing are shown, and a rough comparison with shooting on a regular grid of ray take–off parameters is given.

2 The Two–point Ray Tracing Program

As mentioned above, the principal problem of two–point ray tracing in heterogeneous block models consist in an accurate decomposition of the 2-D ray domain into homogeneous subdomains corresponding to rays of equal ray histories. In the two–point ray tracing program being described, this decomposition is done by means of sophisticated triangularization of the subdomains.

The ray domain is covered gradually by *basic triangles.* (A *triangle* in the ray domain is created by any three rays. A *basic triangle* is an approximately equilateral triangle, the length of its side being given. The apexes of the basic triangle are formed by *basic rays.* A *(in–)homogeneous triangle* is a triangle whose apexes are (not) formed by rays with the same ray history.) Basic triangles serve for the initial estimation of the distribution of homogeneous subdomains in the ray domain as well as for choosing the "working area" where the rays are to be held in the computer memory.

When the new basic triangle is created, the next step is to determine whether it is homogeneous. If it is not, it is necessary to divide this new inhomogeneous basic triangle into homogeneous triangles. First, the *boundary rays* on the sides of the triangle have to be found. (The boundary rays are two very close rays with different values of the ray history. The pairs of boundary rays serve to separate the homogeneous subdomains.) The boundary rays are sought using the method of halving intervals.

The apexes of the triangle together with the boundary rays on its sides are understood to be an *inhomogeneous polygon* from which areas with the same value of the ray history, *homogeneous polygons*, are gradually separated. First, any apex of the inhomogeneous polygon is taken to initiate the homogeneous polygon, together with all its other neighbouring apexes with the same value of the ray history. The boundary between the corresponding ray history and other histories is then traced by pairs of boundary rays in order to complete the homogeneous polygon. Finally, the homogeneous polygon is covered by homogeneous triangles. The method of dividing basic triangles into homogeneous triangles is illustrated in figures 1 to 4. Note that figures 1 to 12 are based on real computation.

The last step of the solution loop of the two-point ray tracing is a search for two-point rays inside (homogeneous) *surface triangles*, formed by the rays incident on the reference surface. The ray which is closest to the receiver on the reference surface is selected, and the parameters of a new ray are proposed using the paraxial ray approximation. If this new ray is closer to the receiver on the reference surface, it becomes a point of departure for proposing a new ray. This procedure is continued until a ray incident sufficiently close to the receiver is found. This ray is then designated as the two-point ray.

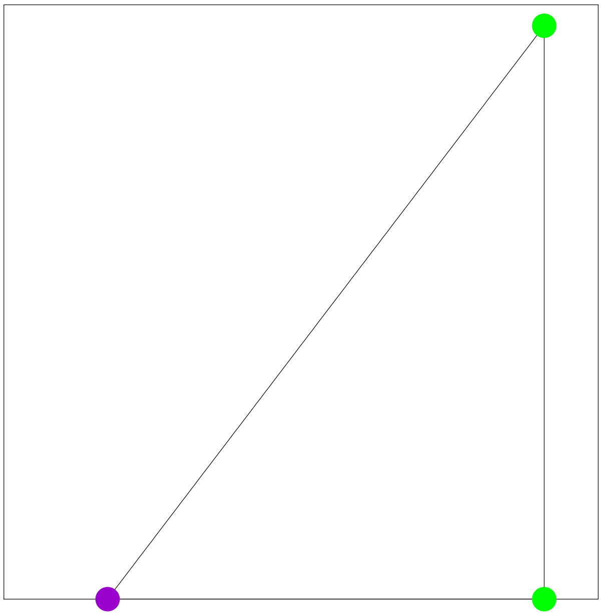

Figure 1. An inhomogeneous basic triangle is formed by basic rays of different ray history. Basic rays are plotted as circles. Rays are colour–coded according to their history.

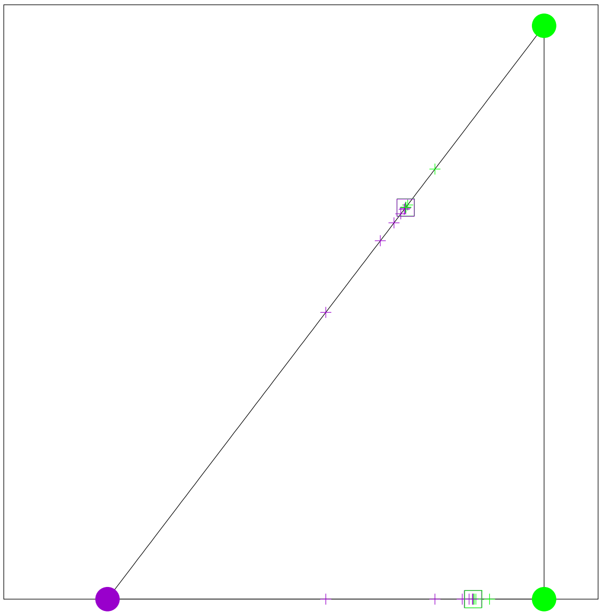

Figure 2. Searching for boundary rays on the sides of the inhomogeneous triangle by halving intervals. Auxiliary rays are plotted as crosses, boundary rays as boxes.

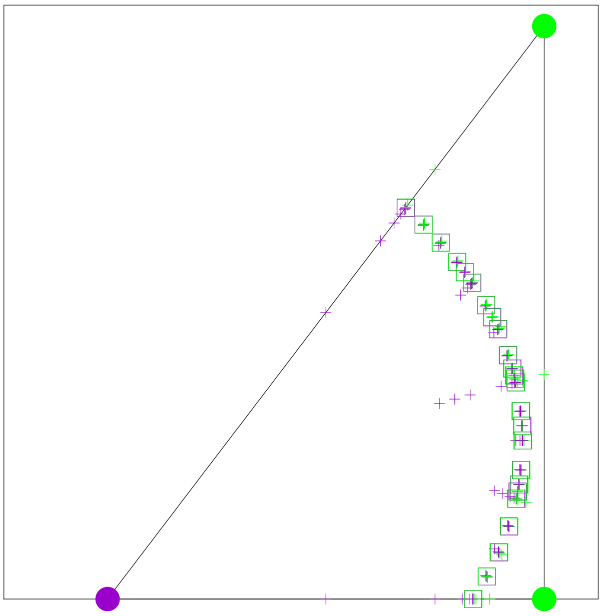

Figure 3. The boundary between the two ray histories is demarcated by pairs of boundary rays. All the boundary rays of the same ray history together with the basic ray(s) create a homogeneous polygon.

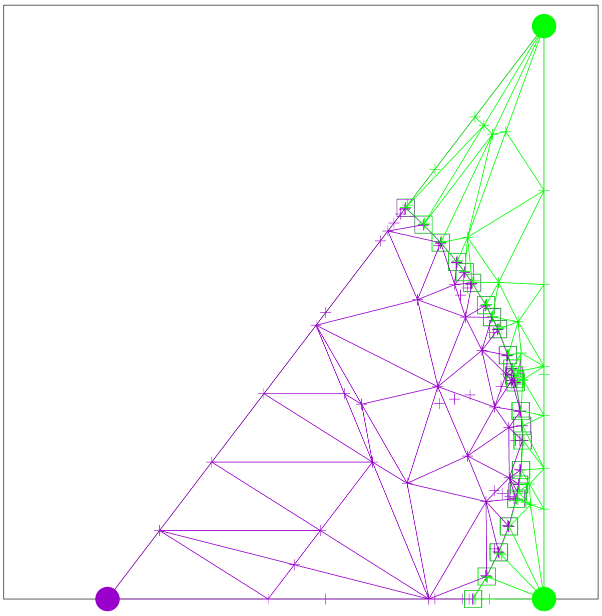

Figure 4. Both homogeneous polygons are covered by homogeneous triangles. Note that the distance between the two boundary rays in each pair is so small that only one box mark can be distinguished.

3 From the Two–point Ray Tracing Program to the Controlled Initial–Value Ray Tracing Program

3.1 Regular Covering of the Reference Surface by Surface Triangles

The final phase of the two–point ray tracing is identifying the two–point rays in the surface triangles. The success of this procedure depends not only on the behaviour of the rays, given by the model and by the initial–value ray tracer, but also on the size of the surface triangles and on their arrangement on the reference surface. The optimum is regular coverage of the reference surface by approximately equilateral surface triangles of the proper and approximately the same size.

As mentioned above, the most important part of the two–point ray tracing consists in a very accurate demarcation of the homogeneous subdomains. In each basic triangle the homogeneous subdomains are first represented by homogeneous polygons, which are then covered by homogeneous triangles. This triangularization may be done in different ways. Because of the nonlinear behaviour of the mapping from the ray domain to the reference surface, different coverages produce different shapes of surface triangles, and the arrangement of surface triangles changes dramatically.

The first difference depends on whether the tracing of the boundary between the different ray histories takes place in the computation. This strongly affects the whole homogeneous polygon, which is to be covered by homogeneous triangles. See figures 5 to 8. The importance of the tracing of the boundary between the different ray histories was discussed in Bulant 1995b and has recently been used in each two–point ray tracing computation.

The second difference is connected with the coverage of the homogeneous polygon by homogeneous triangles. The polygon may either be simply divided into triangles (figures 7 and 8), or covered by approximately equilateral triangles (figures 9 and 10). The coverage of the polygon by triangles requires the computation of several new rays, but usually improves the regularity of the surface triangles. Compare figures 8 and 10.

The regularity of the surface triangles may be improved by dividing surface triangles which are too large. Each side of every surface triangle that is longer than a chosen parameter is halved, and two new triangles are created. This third difference in covering the homogeneous polygon by homogeneous triangles is demonstrated in figures 9 to 12.

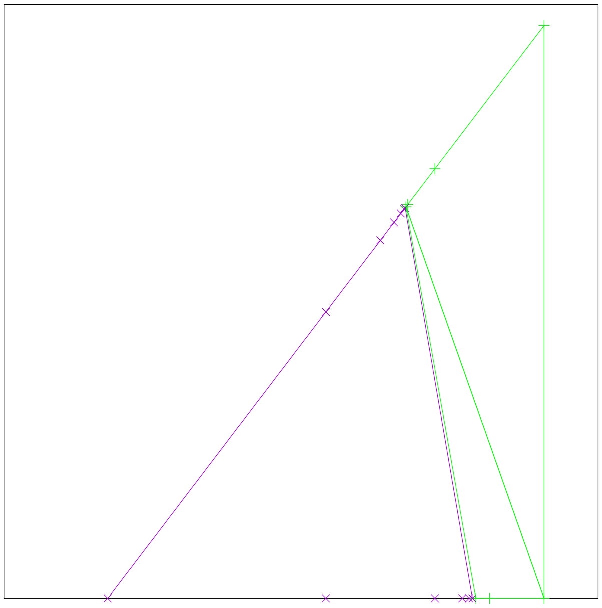

Figure 5. An inhomogeneous basic triangle in the ray domain contains successful rays of two different histories. The basic triangle is simply divided into three homogeneous triangles. The boundary between the two ray histories is not traced. Rays are symbol–coded and colour–coded according to their history.

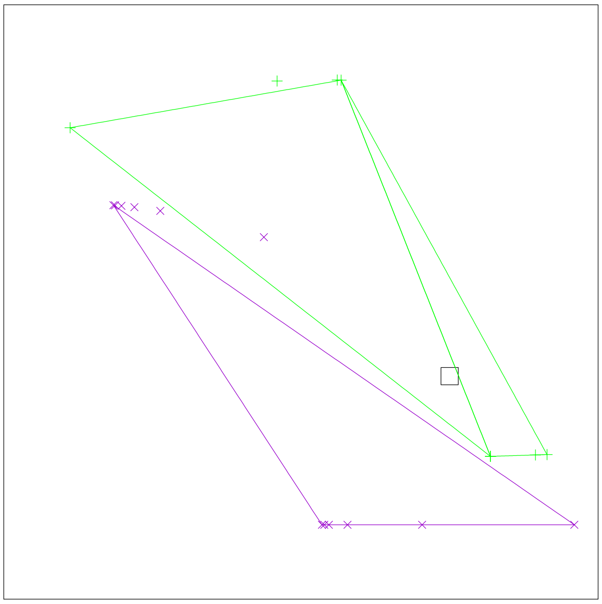

Figure 6. Rays and homogeneous triangles of figure 5 on the reference surface. A receiver (black box) is situated inside one of the surface triangles of green ray history, but the two–point ray to this receiver was not found. Why?

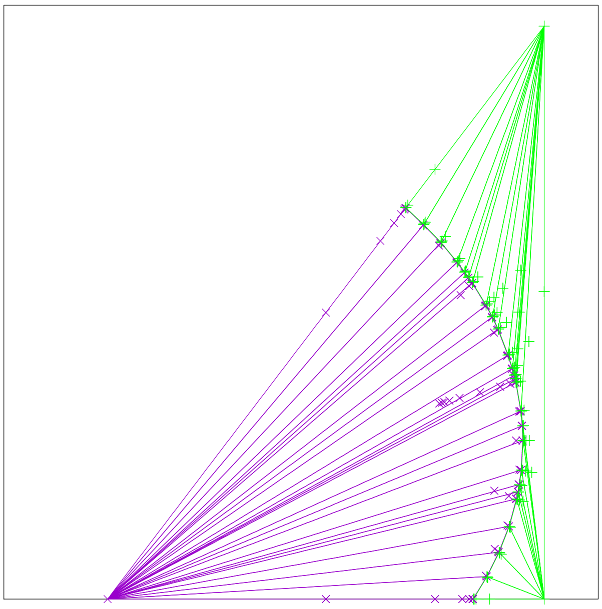

Figure 7. The same basic triangle as in figure 5. The boundary between the two ray histories is now traced, and the triangle is covered by several thin homogeneous triangles.

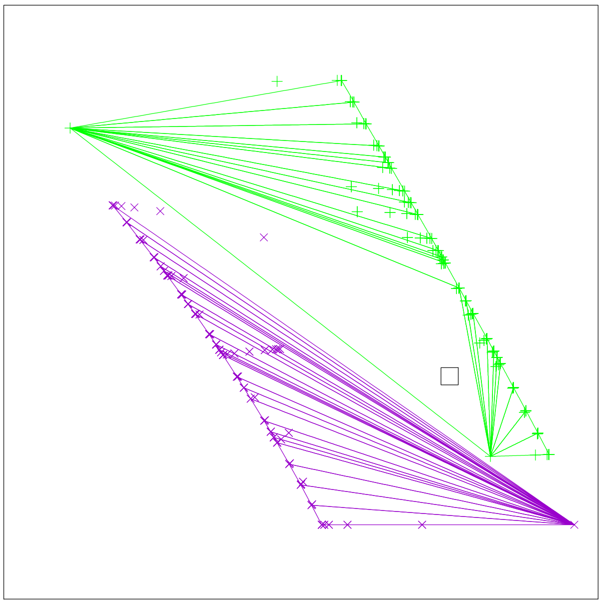

Figure 8. Rays and homogeneous triangles of figure 7 on the reference surface. The two–point ray to the receiver was again not found.

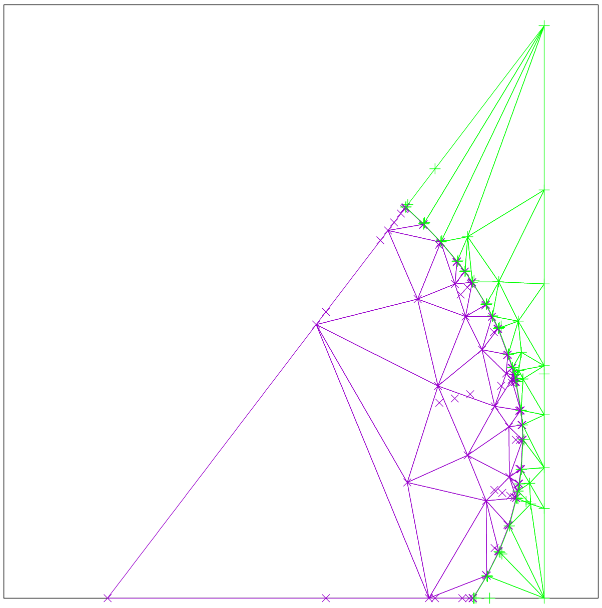

Figure 9. The same basic triangle as in figure 5. The boundary between the two ray histories is now traced, and both subdomains are covered by approximately equilateral homogeneous triangles.

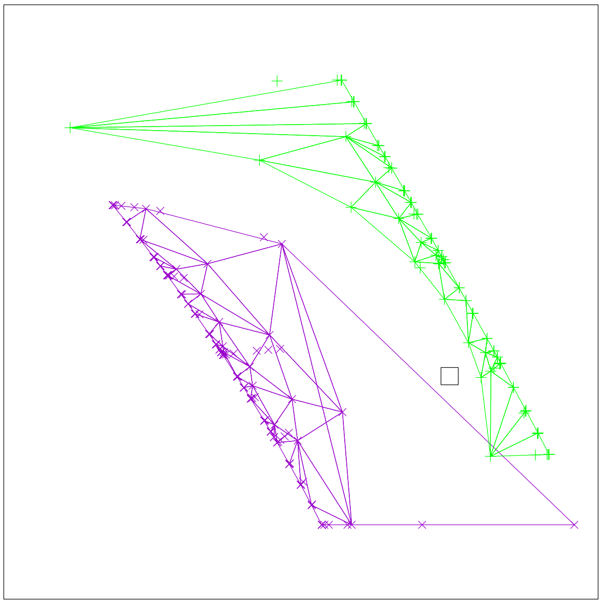

Figure 10. Rays and homogeneous triangles of figure 9 on the reference surface. The receiver is situated outside the surface triangles. Now we can see why any two–point ray of the green history was not found.

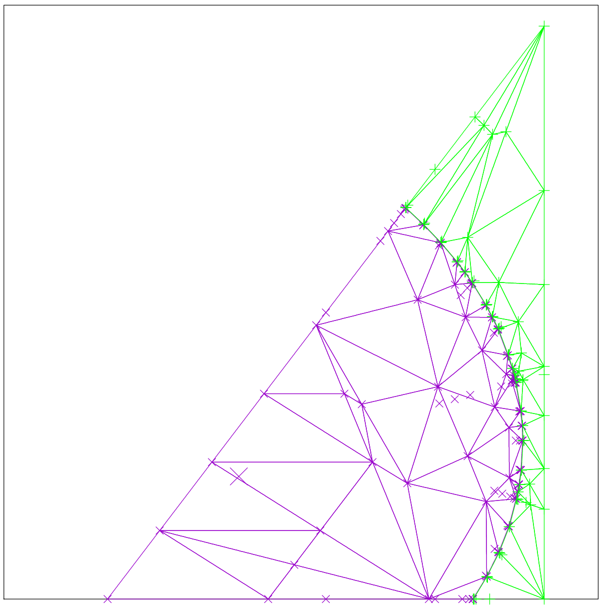

Figure 11. The same basic triangle as in figure 5. The boundary between the two ray histories is traced, the triangle is covered by approximately equilateral homogeneous triangles. All the triangles, which are too large on the reference surface, are divided into smaller ones. One two–point ray of the red history was identified; it is indicated by a larger symbol.

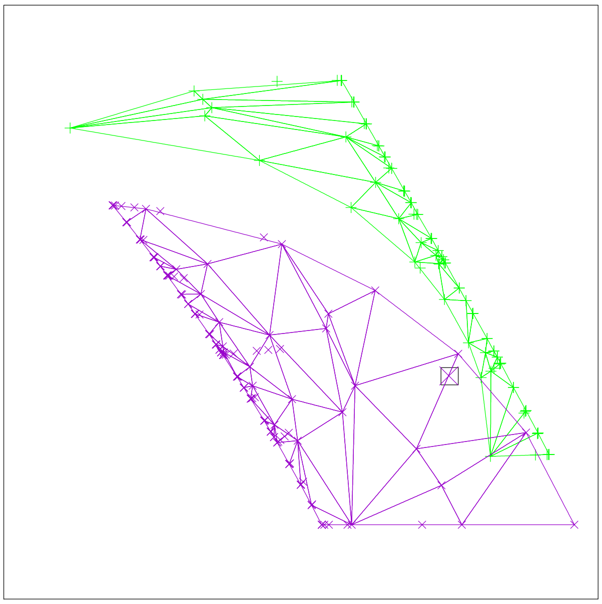

Figure 12. Rays and homogeneous triangles of figure 11 on the reference surface. The receiver is situated inside one of the red surface triangles, a two–point ray of the corresponding history was identified. Compare with figure 6.

3.2 Controlled Initial–Value Ray Tracing

The shooting algorithm, above all based on the procedures of demarcating the boundaries between different ray histories, is thus closely related to *controlled initial-value ray tracing*, whose aim is not to hit given receivers, but to cover the model with a sufficiently dense system of rays (respectively to cover the reference surface with a sufficiently dense system of ray endpoints). The demarcation of ray histories and the triangularization of homogeneous subdomains corresponding to rays of equal ray histories play the principal role in controlled initial–value ray tracing. The space between two consecutive wavefronts is thus decomposed into *ray cells*, as in the *wavefront tracing method* (Vinje *et al.* 1993, 1996a, 1996b), and the travel times and all other calculated quantities may routinely be interpolated within the individual ray cells. Unlike the *weighting of paraxial ray approximations*, this method is capable of strictly complying with the boundaries of shadow zones. Controlled initial–value ray tracing, basically equivalent to wavefront tracing, is thus a very promising tool for fast calculation of most energetic *elementary travel times* at gridpoints of dense rectangular grids of points for, e.g., ray–theory based migration techniques, or the nonlinear determination of seismic hypocentres.

In wavefront tracing, the mutual distance of the rays is controlled in the whole model volume. In controlled initial–value ray tracing it is controlled only inside the homogeneous subdomains corresponding to the successful rays. Thus the number of computed rays need not be higher in controlled initial–value ray tracing than in wavefront tracing.

Inside the homogeneous subdomains corresponding to successful rays, the total length of the traced rays may be about three times shorter in wavefront tracing than in controlled initial–value ray tracing. On the other hand, in wavefront tracing the rays are traced by parts, which may slow down tracing, corresponding to the difference between the Runge–Kutta and Hamming's predictor–corrector methods, sometimes even more than twice. Thus the speed of wavefront tracing need not be much higher than that of controlled initial–value ray tracing.

4 Numerical Examples

A three–layer seismic model is used as the first numerical example of using the two–point ray tracing program. The model is composed of the plane Earth surface and two three–dimensional interfaces. The uppermost layer has a constant vertical velocity gradient, the velocity in the middle layer is laterally varying with a vertical gradient higher than the gradient in the uppermost layer. Lateral variations of the velocity are about twice larger than the vertical gradient. The lowermost layer has a constant (and highest) seismic P-wave velocity. The dimensions of the model are approximately 8 x 9.4 x 3 km.

The receivers form a linear profile on the plane Earth surface, where the point source is also situated. Only the rays corresponding to the elementary wave reflected at the lower interface are taken into account in the computation. The model and the computed two–point rays are illustrated in figure 13.

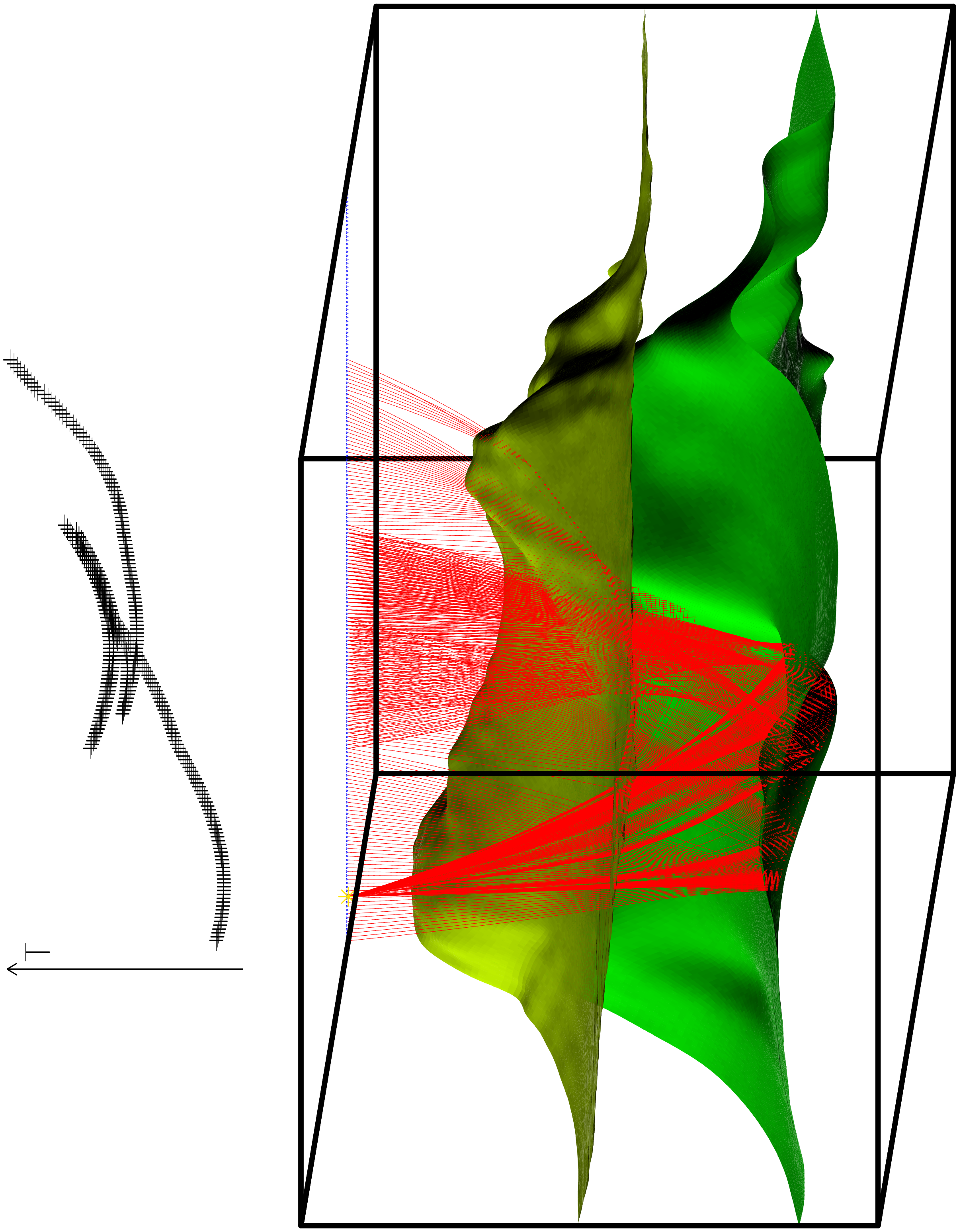

Figure 13. The three–layer model used as a numerical example of the two–point ray tracing with the two–point rays identified during the computation. A yellow asterisk represents the point source, the small blue triangles are the receivers.

The time curve above the model demonstrates the relative travel times of the two–point rays identified.

The shooting parameters are chosen so hat the first parameter corresponds approximately to the angle between the ray and plane xz, and the second to the angle between the ray and plane yz, where x and y are the horizontal axes and z is the vertical axis. The ray domain of the computation in terms of shooting parameters ranges from -0.05 π to 0.6 π in the direction of the receiver profile, and from -0.17 π to 0.12 π perpendicularly to the profile. 40331 rays with 9 different ray histories are computed and 410 two–point rays are found. The computer time required on a PC Pentium 90 Mhz is 1 hour and 5 minutes. Figure 14 displays the coverage of the ray domain by seismic rays.

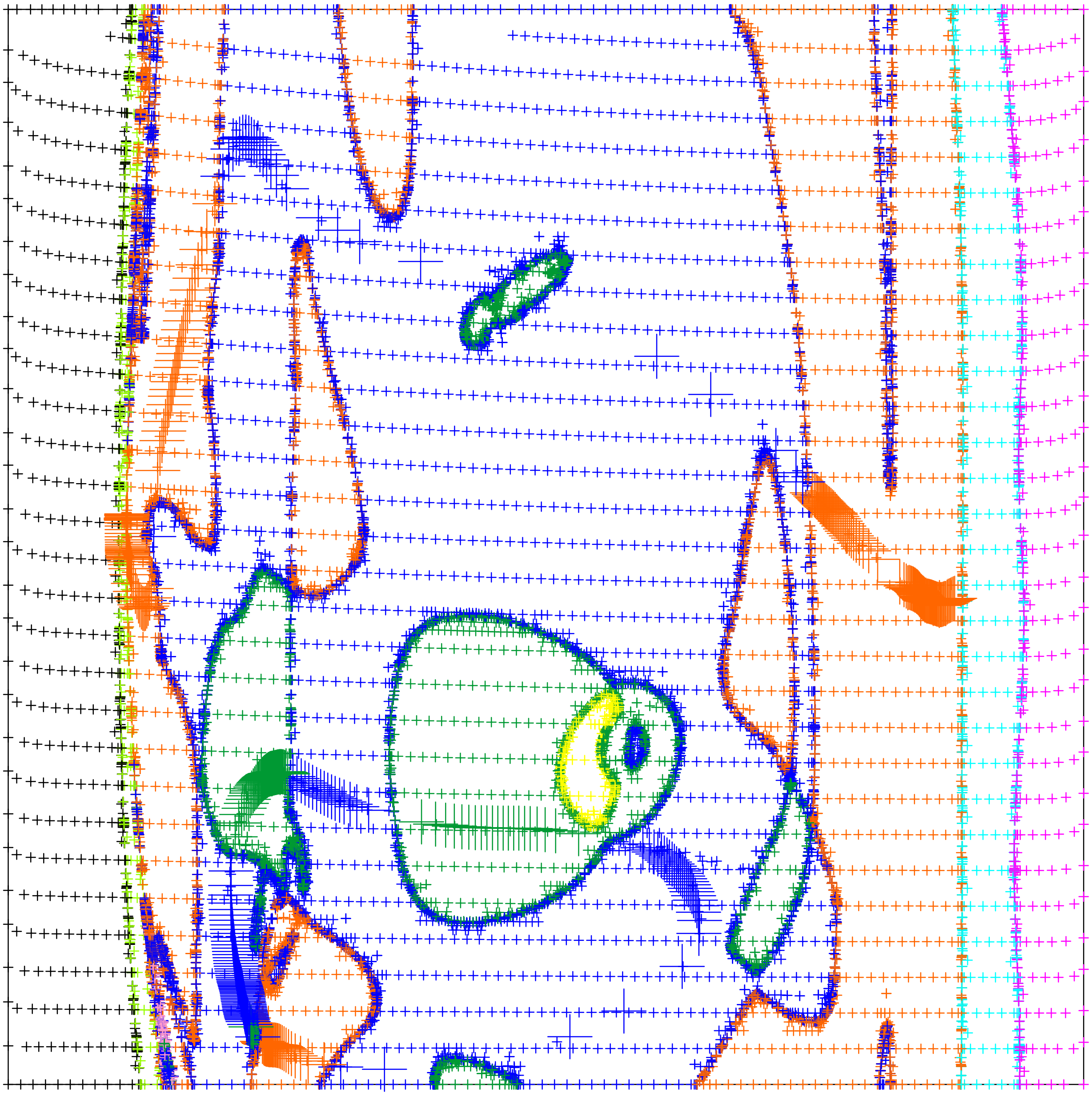

Figure 14. The coverage of the ray domain by seismic rays shot during the computation. The rays are colour–coded according to the ray history, two–point rays are plotted as larger crosses. The mutual distances between two neighbouring two–point rays of the same history provide interesting information about the geometrical spreading inside corresponding homogeneous subdomains.

In the computation the reference surface (plane Earth surface) is covered by homogeneous triangles with sides of maximum length 2 km. The configuration of these homogeneous triangles of single selected ray history on the reference surface is shown in figure 15.

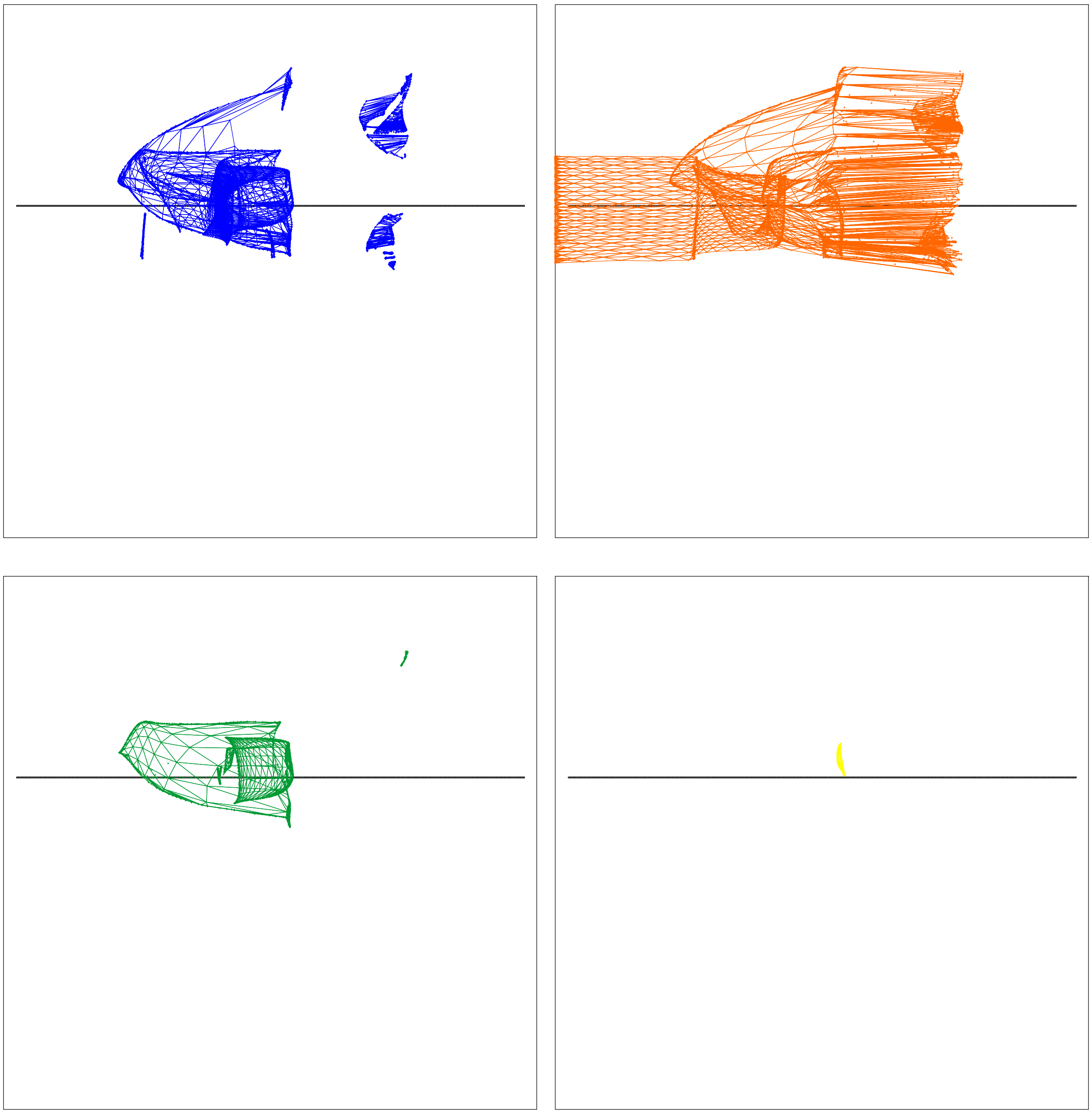

Figure 15. The coverage of the reference surface by seismic rays and homogeneous triangles of one selected ray history shot and created during the computation. The rays and triangles are colour–coded according to the ray history, the same colours as in figure 14 are used. The bold black line denotes the receiver profile.

The second numerical example of two-point ray tracing in 3-D is the computation of a diffracted elementary wave in a model with a lens. The two-layer model with a smooth 2,5-D Earth surface and first–order structural interface has a homogeneous lenticular inclusion in the upper constant velocity gradient layer. The lenticular inclusion has a higher velocity than its neighbourhood, and the velocity is highest in the lower layer. The dimensions of the model are: length 60 km, width 40 km, and height 30 km, including the free space. The model is the demo model of the MODEL package.

Two-point ray tracing is performed for the point source and elementary wave diffracted at the edge of the lenticular inclusion, receivers form a linear profile on the curved Earth surface. The computation of the diffracted wave is stepwise.

In the first step, the edge is understood to be a set of receivers, and two–point rays are computed from the point source to the receivers (to the edge). Only the rays corresponding to the refracted elementary wave are taken into account in this numerical example. See figure 16.

The rays of one single history computed in the first step are chosen in the second step. These are rays, which propagated through the lens, but they might be also the direct rays. The edge diffractor is now understood to be a linear source, the initial travel time is interpolated using the travel times of the chosen two–point rays. Note that the ray domain of the linear source is again 2-dimensional, the first ray take–off parameter is the length along the edge, and the second is the shooting angle. One selects the elementary wave to be computed (in the presented example this is the refracted wave), and the two-point rays from the edge to the receiver profile are traced. See figure 17. The travel times of the rays leaving the point source, diffracted at the edge, and reaching the receivers are now available.

The third step is similar to the first. The rays from the point source to the points of departure of the two–point rays, computed in the second step, are traced. Only the rays of the history selected in the second step are taken into account. The third step is carried out only for plotting purposes, to be able to display the final picture of the diffracted rays — figure 18.

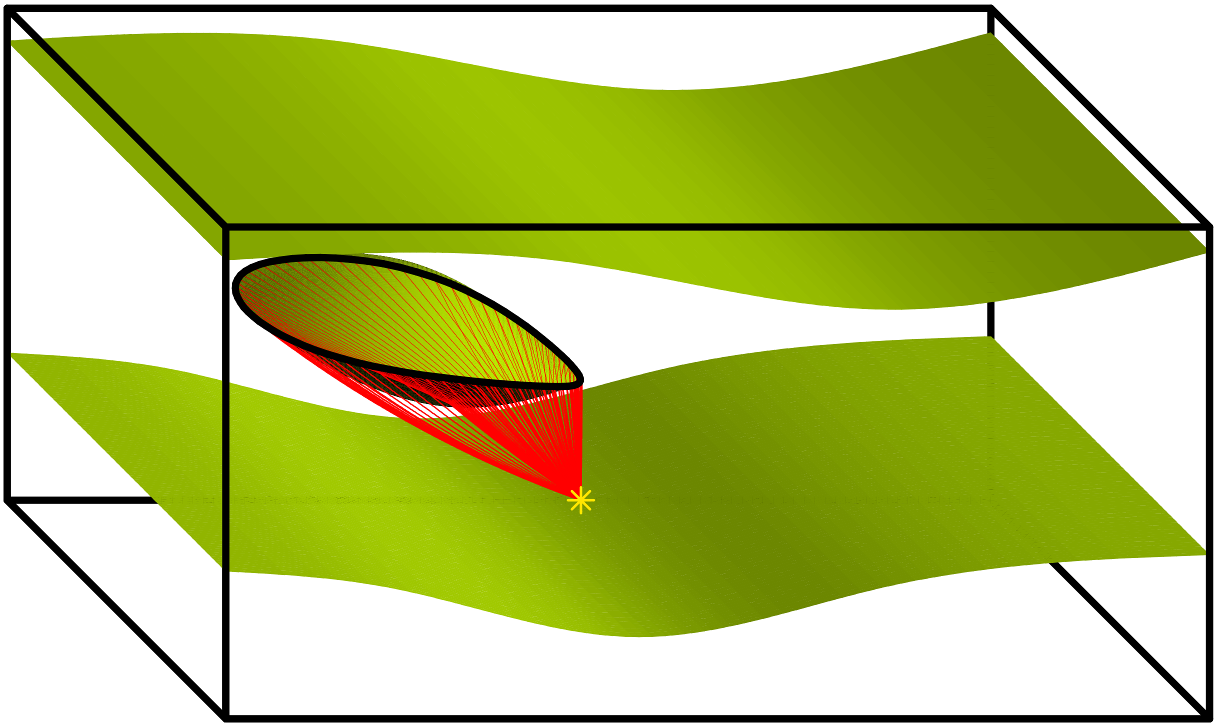

Figure 16. First step of the computation of diffracted rays in the model with lens. The rays from the point source to the edge of the lenticular inclusion are computed. Only refracted rays are considered. The yellow asterisk represents the point source, the blue dots are the receivers, placed along the edge.

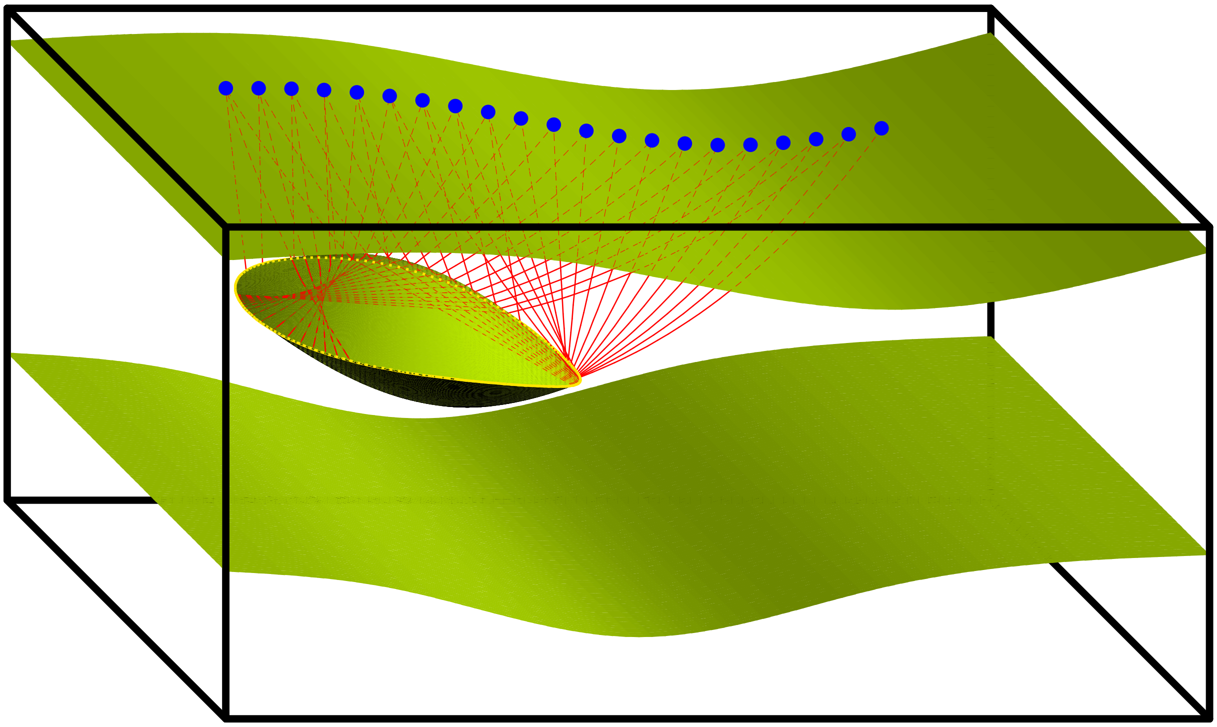

Figure 17. The second step of the computation of diffracted rays in the model with the lens. The rays from the edge of the lenticular inclusion to the receivers are computed. Only refracted rays are considered. The yellow line represents the edge diffractor, the blue dots are the receivers.

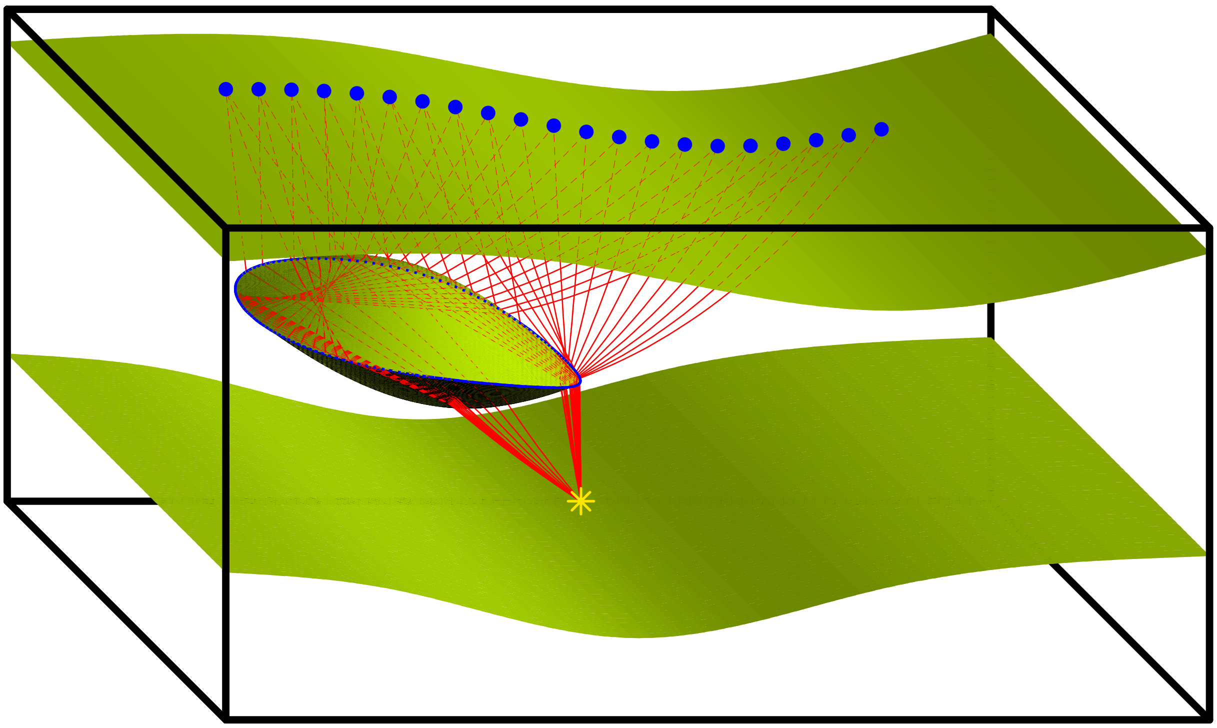

Figure 18. Final result — the two-point rays leaving the point source, refracted through the lens, diffracted at the edge of the lenticular inclusion, and reaching receivers without reflection at any interface are computed. The yellow asterisk represents the point source, the blue dots are the receivers.

5 Conclusions

The algorithm for two-point ray tracing in a 3-D heterogeneous medium has been developed. Special emphasis was put on the sufficiently accurate determination of the boundaries between rays with different ray histories, and on finding all the homogeneous subdomains of the ray domain. Consequently, the algorithm is very reliable in computing all two-point rays of the given elementary waves to the given receivers.

The two-point ray tracing program described is relatively demanding with regard to the number of rays to be traced. The number of rays, which have to be computed, is not significantly affected by the number of receivers, because these mostly involve auxiliary rays required to divide the domain of the ray take–off parameters into regions with the same value of the ray history. The method is highly reliable in finding two–point rays in very thin regions of the ray domain. This might be of interest for, e.g., 3-D tomography in smooth models, or for interpretation and model verification purposes.

In each computation, the width of the demarcation belts is kept below some prescribed limit. This enables to roughly estimate about the number of rays which should be traced in shooting on a regular rectangular grid of ray take–off parameters, if the width of the demarcation belts should be approximately the same as in the two–point ray tracing described:

Computation in the three-layer model:

- Dimension of the ray domain: 100×30 units
- Given maximum distance between two rays of different histories forming a pair of boundary rays: 0.002 units
- Regular–grid initial–value ray tracing:
  $(100/0.002)\times(30/0.002) = 50\ 000\times15\ 000 =$ **750 000 000** rays
- Shooting program described: **40 331** rays

The designed shooting algorithm, is closely related to controlled initial–value ray tracing, which seems to be a promising tool for the fast calculation of elementary travel times, e.g., for ray-theory based migration techniques, or the nonlinear determination of seismic hypocentres.

References

Bulant, P. (1996): Two–point ray tracing in 3-D. PAGEOPH, in press.

Bulant, P. (1995a): Two–point ray tracing in 3-D. In: Seismic Waves in Complex 3-D Structures, Report 3, pp. 37-64, Department of Geophysics, Charles University, Prague.

Bulant, P. (1995b): Numerical examples of two–point ray tracing in 3-D. In: Seismic Waves in Complex 3-D Structures, Report 3, pp. 65-92, Department of Geophysics, Charles University, Prague.

Červený, V., Klimeš, L. & Pšenčík, I. (1988): Complete seismic–ray tracing in three–dimensional structures. In: Doornbos, D.J. (ed.), Seismological Algorithms, pp. 89–168. Academic Press, New York.

Vinje, V., Iversen, E. & Gjøystdal, H. (1993): Traveltime and amplitude estimation using wavefront construction. Geophysics, **58**, 1157–1166.

Vinje, V., Iversen, E., Gjøystdal, H. & Åstebøl, K. (1996a): Estimation of multivalued arrivals in 3D models using wavefront construction — Part I. Geophys. Prospecting, **44**, 819–842.

Vinje, V., Iversen, E., Gjøystdal, H. & Åstebøl, K. (1996b): Part II: Tracing and interpolation. Geophys. Prospecting, **44**, 843–858.